integration of absorptivity over height. We calculated the brightness temperature spectrum according to the method of Ho *et al.* (*7*), adding the contribution from the isothermal layer below z_i. We calculated the polarized interferometric visibility as Clark and Kuz'min did (*12*, eq. A3). Furthermore, within this model, the altitude of a reference temperature (taken as 450°K) measured by Mariner V at a distance of 6085 ± 2 km from the center of Venus determines the planetary radius.

The most likely values of T_s and z_i, the variable parameters of our model, are then obtained by calculating the weighted sum of the squares of the deviation of all items enumerated in the preceding paragraph. The square of the deviation of calculated values from their corresponding experimental values is divided by the variance of each set of experimental data. The brightness temperature spectrum and visibility curve and the single "points" of optical depth and planetary radius are treated equally by dividing the sum of squares for the respective curve by the number of points taken along that curve. The weighted sum of the squared deviations reaches its minimum with $T_s = 670° \pm 20°$K and $z_i = 7 \pm 2$ km. These values yield $\tau_0 = 15.4$; a planetary radius $R =$ 6054.8 km as compared to a value of 6050 to 6056 km obtained from radar echo delay (*13*); polarized interferometric visibility ΔF (wavelength $\lambda = 10.6$ cm, normalized base line length $\beta = 0.6) = 5.5$ percent [Clark and Kuz'min (*12*) reported a value of 5.6 ± 1 percent]; the brightness temperature spectrum based on the most likely values of T_s and z_i is presented in Fig. 2.

Figure 2 also presents the brightness temperature derived from an adiabatic temperature profile investigated by setting z_i equal to 0. With this value of z_i, the surface temperature minimizing the weighted sum of the squared deviations is $T_s = 720° \pm 20°$K. Other results of this model are $\tau_0 = 12.6$, $R =$ 6055.5 km, and ΔF ($\lambda = 10.6$ cm, $\beta = 0.6) = 6.3$ percent. The weighted sum of the squared deviations is, however, about two and one-half times greater than that obtained with the above isothermal model.

The best fit of all data is thus obtained with the isothermal model. Current interferometric observations of Venus at 11 cm should permit refined measurement of polarized interferometric visibility and yield the unpolarized visibility with sufficient accuracy to enable one to distinguish between the models. Simultaneous measurement of the radar cross section of Venus at several frequencies can be expected to yield greatly improved estimates of microwave optical depth.

W. GALE, M. LIWSHITZ
A. C. E. SINCLAIR
Bellcom, Inc., Washington, D.C.

References

1. A. Kliore, G. S. Levy, D. L. Cain, G. Fjeldbo, S. I. Rasool, *Science* **158**, 1683 (1967).
2. V. S. Avduevsky, M. Yu. Marov, M. K. Rozhdestvensky, *J. Atmos. Sci.* **25**, 533 (1968).
3. R. P. Ingalls, R. A. Brockelman, J. V. Evans, J. I. Levine, G. H. Pettengill, L. P. Rainville, A. E. E. Rogers, F. S. Weinstein, *Lincoln Lab. Tech. Rep. No. 456* (1968).
4. R. L. Carpenter, *Astron. J.* **71**, 142 (1966).
5. G. H. Pettengill, R. B. Dyce, D. B. Campbell, *ibid.* **72**, 330 (1967).
6. J. R. Dickel, *Icarus* **6**, 417 (1967); J. R. Dickel, W. W. Warnock, W. J. Medd, *Nature* **220**, 1183 (1968); D. Barber and H. Gent, *Planet. Space Sci.* **15**, 907 (1967).
7. W. Ho, I. A. Kauffman, P. Thaddeus, *J. Geophys. Res.* **71**, 5091 (1966).
8. A. T. Wood, Jr., R. B. Wattson, J. B. Pollack, *Science* **162**, 114 (1968).
9. W. Gale and A. C. E. Sinclair, in preparation.
10. I. I. Shapiro, *Science* **157**, 423 (1967).
11. P. Thaddeus, *J. Atmos. Sci.* **25**, 665 (1968); personal communication.
12. B. G. Clark and A. D. Kuz'min, *Astrophys. J.* **142**, 23 (1965).
13. M. E. Ash, R. P. Ingalls, E. H. Pettengill, I. I. Shapiro, W. B. Smith, M. A. Slade, D. B. Campbell, R. B. Dyce, R. Jurgens, T. W. Thompson, *J. Atmos. Sci.* **25**, 560 (1968).

25 March 1969

Cyclic and Geographic Trends in Seawater Temperature and Abundance of American Lobster

Abstract. *In Maine, fluctuations in the abundance of American lobster* (Homarus americanus) *and in seawater temperature have correlated well during the years since the first temperature measurements were made in 1905. Recent record catches in chronological sequence from the northern limit of range in Newfoundland to New York, while temperatures measured in Maine declined from higher to lower than optimum, suggest that at the present rate optimum conditions should reach the southern limit of the lobster's range by the mid-1970's.*

The temperature of the sea surface, as measured daily since 1905 at Boothbay Harbor, Maine, by the U.S. Fish and Wildlife Service, has fluctuated as distinct climatic subcycles, including (i) the years before 1917, (ii) the period from 1917 to 1939, and (iii) the years since 1939 (Fig. 1) (*1*).

The period since 1939 has been of special biological and meteorological interest. The second coldest year on record, 1939, terminated a relatively low-temperature subcycle that had commenced in 1917; it also initiated a 14-year warming trend that culminated in the record high of 11.1°C in 1953 which, in turn, was followed by an equally precipitate decline, reaching an average of 7.3°C by 1967.

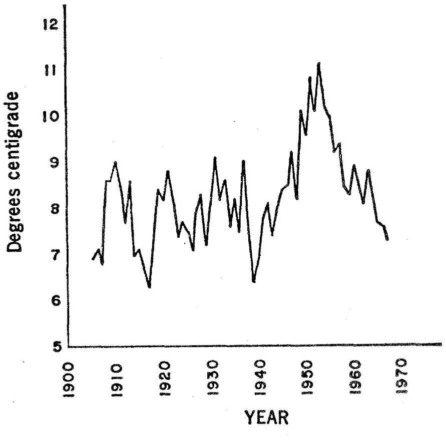

Fig. 1. Sea surface temperature (Boothbay Harbor, Maine) measured by U.S. Fish and Wildlife Service, 1905–1967. (Temperature means for 1905, 1948, and 1949 were estimated from 9, 11, and 8 months, respectively.)

Temperature data as indicators of climatic trends appear to be consistent with sea surface temperature variations recorded elsewhere along the northwest Atlantic coast (*2*). It is assumed that temperature fluctuations at Boothbay Harbor are representative of climatic trends throughout the range of the American lobster (*3*) and that the 28 percent contribution of Maine to the catch for the period from 1939 to 1967 is reasonably representative of resource behavior in terms of both abundance and availability (Fig. 2).

A linear correlation of .8 between lobster production in Maine and elsewhere for the period from 1939 to 1967 supports the assumption that factors causing fluctuations in Maine landings also influence yield elsewhere (Fig. 3). From the 6.4°C annual mean in 1939, when relatively high production occurred in Connecticut and a record high catch was made in Rhode Island, a northeasterly trend in greater yield of the traditional American lobster trap fishery developed coincident with the 14-year cycle of the increasing temperature of the sea surface. The increase in

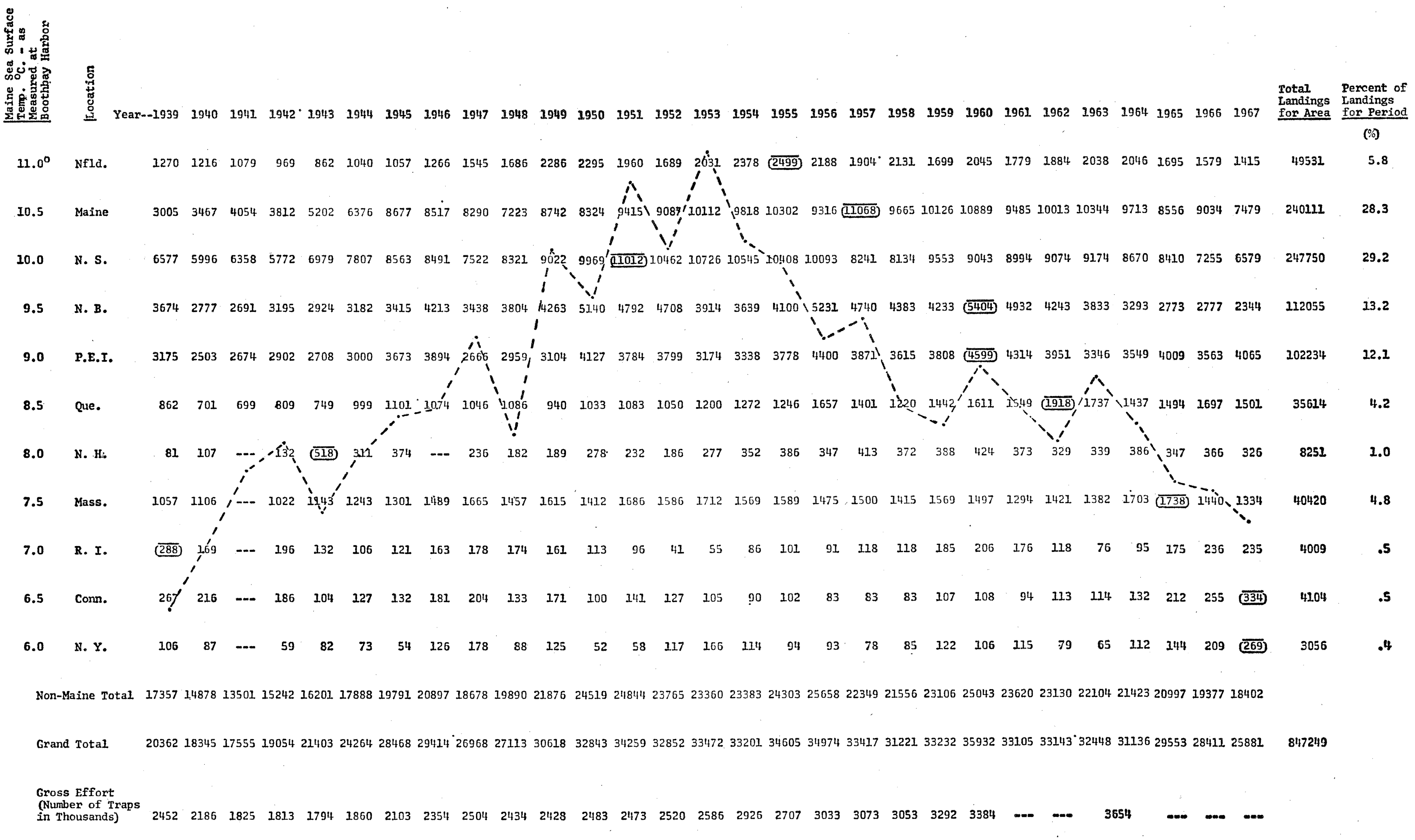

Maine Sea Surface Temp. °C. – as Measured at Boothbay Harbor	Location	Year--1939	1940	1941	1942	1943	1944	1945	1946	1947	1948	1949	1950	1951	1952	1953	1954	1955	1956	1957	1958	1959	1960	1961	1962	1963	1964	1965	1966	1967	Total Landings for Area	Percent of Landings for Period (%)
11.0°	Nfld.	1270	1216	1079	969	862	1040	1057	1266	1545	1686	2286	2295	1960	1689	2031	2378	(2499)	2188	1904	2131	1699	2045	1779	1884	2038	2046	1695	1579	1415	49531	5.8
10.5	Maine	3005	3467	4054	3812	5202	6376	8677	8517	8290	7223	8742	8324	9415	9087	10112	9818	10302	9316	(11068)	9665	10126	10889	9485	10013	10344	9713	8556	9034	7479	240111	28.3
10.0	N. S.	6577	5996	6358	5772	6979	7807	8563	8491	7522	8321	9022	9969	(11012)	10462	10726	10545	10408	10093	8241	8134	9553	9043	8994	9074	9174	8670	8410	7255	6579	247750	29.2
9.5	N. B.	3674	2777	2691	3195	2924	3182	3415	4213	3438	3804	4263	5140	4792	4708	3914	3639	4100	5231	4740	4383	4233	(5404)	4932	4243	3833	3293	2773	2777	2344	112055	13.2
9.0	P.E.I.	3175	2503	2674	2902	2708	3000	3673	3894	2666	2959	3104	4127	3784	3799	3174	3338	3778	4400	3871	3615	3808	(4599)	4314	3951	3346	3549	4009	3563	4065	102234	12.1
8.5	Que.	862	701	699	809	749	999	1101	1074	1046	1086	940	1033	1083	1050	1200	1272	1246	1657	1401	1220	1442	1611	1549	(1918)	1737	1437	1494	1697	1501	35614	4.2
8.0	N. H.	81	107	---	132	(518)	311	374	---	236	182	189	278	232	186	277	352	386	347	413	372	388	424	373	329	339	386	347	366	326	8251	1.0
7.5	Mass.	1057	1106	---	1022	1143	1243	1301	1489	1665	1457	1615	1412	1686	1586	1712	1569	1589	1475	1500	1415	1569	1497	1294	1421	1382	1703	(1738)	1440	1334	40420	4.8
7.0	R. I.	(288)	169	---	196	132	106	121	163	178	174	161	113	96	41	55	86	101	91	118	118	185	206	176	118	76	95	175	236	235	4009	.5
6.5	Conn.	267	216	---	186	104	127	132	181	204	133	171	100	141	127	105	90	102	83	83	83	107	108	94	113	114	132	212	255	(334)	4104	.5
6.0	N. Y.	106	87	---	59	82	73	54	126	178	88	125	52	58	117	166	114	94	93	78	85	122	106	115	79	65	112	144	209	(269)	3056	.4
	Non-Maine Total	17357	14878	13501	15242	16201	17888	19791	20897	18678	19890	21876	24519	24844	23765	23360	23383	24303	25658	22349	21556	23106	25043	23620	23130	22104	21423	20997	19377	18402		
	Grand Total	20362	18345	17555	19054	21403	24264	28468	29414	26968	27113	30618	32843	34259	32852	33472	33201	34605	34974	33417	31221	33232	35932	33105	33143	32448	31136	29553	28411	25881	847249	
	Gross Effort (Number of Traps in Thousands)	2452	2186	1825	1813	1794	1860	2103	2354	2504	2434	2428	2483	2473	2520	2586	2926	2707	3033	3073	3053	3292	3384	---	---	3654		---	---	---		

( ) Record high landings during period 1939-1967

•------• Approximate trace of sea surface temp. trend °C.

Fig. 2. American lobster landings in metric tons (trap landings only).

Table 1. Decade-interval changes in fishing effort in thousands of traps and in percent.

Area	Traps 1944 (No.)	Traps 1954 (No.)	Change (%)	Traps 1964 (No.)	Change (%)	Total change 1944–1964 (%)	Maximum catch year
Newfoundland		286		550	+92.0	+92.0	1955
New Brunswick	326	428	+31.3	546	+27.6	+67.5	1960
Prince Edward Island	292	417	+42.8	524	+25.7	+79.5	1960
Nova Scotia	826	1054	+27.6	1180	+12.0	+42.9	1951
Quebec	82	113	+37.8	139	+23.0	+69.5	1962
Maine	252	488	+93.7	754	+54.5	+199.2	1957
New Hampshire	9	14	+55.6	17	+21.4	+88.9	1943
Massachusetts	46	99	+115.2	107	+ 8.1	+132.6	1965
Connecticut	11	8	−18.1	7	−12.5	−36.4	1967
Rhode Island	9	12	+33.3	10	−16.7	+11.1	1939
New York	6	8	+33.3	6	−25.0	0	1967

trap catch from south to north followed record low yields for the period in New Hampshire and Maine in 1939, Prince Edward Island in 1940, Quebec and New Brunswick in 1941, Nova Scotia in 1942, and Newfoundland in 1943 (Fig. 2) (*4*).

As temperatures rose after 1939, the record low production of the northern areas was rapidly displaced by high yields beginning with New Hampshire in 1943 and moving progressively north and east to Newfoundland, the northern terminus of the lobster's range. During this time, record low trap catches were made in New York, Rhode Island, and Connecticut, and even farther south, apparently because of higher-than-optimum sea temperature (*5*). Generally high levels of yield were sustained throughout the areas north and east of Rhode Island, ranging from 16 years in Newfoundland to 22 years in New Hampshire and Massachusetts.

With the decline in temperature after 1953, record high lobster catches occurred in a generally north to south direction from Newfoundland in 1955 to Connecticut and New York in 1967. Presumably, each growing area was exposed to optimum temperatures during both the northward and southward drift. Peak fishing effort during the period of optimum temperatures determined the year of maximum catch (Table 1). From the end of World War II through 1956, increases of 40 percent in effort and 12½ percent in yield in Maine absorbed all but 14 percent of the available legal supply. It is presumed that comparable relations between effort and yield occurred elsewhere, modified as they were in Maine by fluctuations in sea temperature.

After 1944, increases in fishing effort, as measured by the number of traps being fished, occurred principally in Maine, Massachusetts, and Newfoundland (Table 1). It is evident that a marked increase in the number of traps fished in nearly all areas did not prevent a substantial decline in catch throughout the northern portion (Newfoundland to Massachusetts) of the lobster range in the middle and late 1960's, coincident with a decline in sea surface temperature.

Although a correlation of .9 from 1897 to 1960 between fishing effort and annual catch in Maine (*6*) indicates the influence of effort on yield of the fishery, after 1956 effort and catch are inversely related in the Maine fishery as well as in the Newfoundland to New York fisheries.

Within the Massachusetts to Newfoundland area, average lobster production increased 60 percent and effort 75 percent during the years of optimum temperature. After the optimum temperature period ended, catch declined 12½ percent despite an average 20 percent increase in effort in those areas where data are available.

As conditions suitable for record high production have moved southwesterly into southern New England and New York, new record lows occurred in several northern areas—in New Brunswick the smallest annual catch within the 1939 to 1967 period, in Newfoundland a 21-year low, in Nova Scotia the lowest production since 1941, and in Maine a 19-year minimum.

In view of the association of climatic trends with the magnitude of inshore lobster populations and the present rate of decline in sea surface temperature, it is likely that optimum condi-

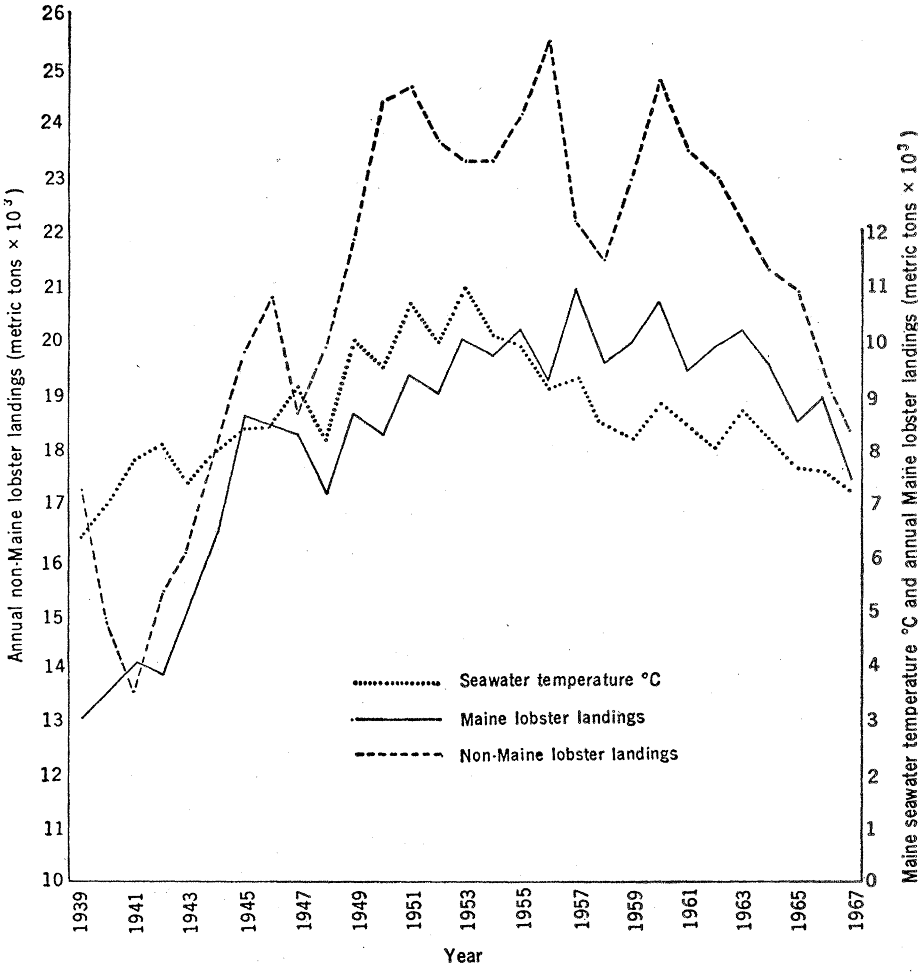

Fig. 3. Comparison of Maine and non-Maine lobster landings with Boothbay Harbor sea surface temperature.

tions will reach the southern limit of the lobster's range in the vicinity of Cape Hatteras during the middle 1970's.

Cyclic and geographic trends in lobster abundance and demonstrated fluctuations in other commercially important populations with climatic trends serve to identify probable maximum limits of inshore marine resource yield under natural conditions.

ROBERT L. DOW
Department of Sea and Shore Fisheries, Augusta, Maine 04330

References and Notes

1. W. Welch, *Monthly and Annual Means of Surface Seawater Temperature, Boothbay Harbor, Maine, 1905 through 1966* (U.S. Bureau of Commercial Fisheries, Boothbay Harbor, Maine, 1967).
2. L. M. Lauzier, *Special Publication No. 6* (International Commission for the Northwest Atlantic Fisheries Environmental Symposium, Rome, 1964).
3. H. C. Willett and J. T. Prohaska, *Final Scientific Report, NSF Grant 14077* (Cambridge, Mass., 1 Oct. 1963).
4. *Monthly Review of Canadian Fisheries Statistics, 1964 to 1968* (Dominion Bureau of Statistics, Ottawa), vols. 1 to 21.
5. *Fishery Statistics of the United States, 1921 to 1967* (U.S. Bureau of Commercial Fisheries, Dept. of Interior, Washington, D.C.).
6. R. L. Dow, *Commer. Fish. Rev.* **23** (9), 1 (Sept. 1961).
7. I thank Hurd Willett of the Dept. of Meteorology, M.I.T., for advice and comments on climatic trends; D. G. Wilder, Fisheries Research Board of Canada, St. Andrews, N.B., for catch data from the Canadian Provinces; and Charles Lyles of the U.S. Fish and Wildlife Service for differentiated data on U.S. lobster landings.

13 February 1969

■

Basic Ferric Phosphates: A Crystallochemical Principle

Abstract. *A polyatomic complex of iron-oxygen octahedral face-sharing triplets corner-linked to four other octahedra occurs in the atomic arrangements of the basic iron phosphates dufrenite, rockbridgeite, beraunite, and laubmannite. This complex is further knit together by the phosphate tetrahedra. The family of basic ferric phosphates arises from the variety of ways in which the complexes can be linked along a third "variable" crystallographic axis.*

The basic ferric phosphates, perplexing substances in the mineral kingdom, occur as replacements of organic products, such as wood and bones; as nodules in marls and soils; as secondary minerals in "limonite" beds and deposits of iron ore; and as hydrothermally reworked products of primary lithium-iron-manganese phosphates in pegmatites. Conflict and contradiction have frequently appeared in the nomenclature and data reported for these phosphates. Frondel (*1*) presented a historical survey as well as information on the physical and chemical characters of these minerals. Fanfani and Zanazzi (*2*) reported on the atomic arrangement of one member, beraunite.

The basic ferric phosphates include the species dufrenite $[Fe_3(OH)_3(H_2O)(PO_4)_2]$, rockbridgeite $[Fe_5(OH)_4(O)(PO_4)_3]$, laubmannite $[Fe_9(OH)_{15}(PO_4)_4]$, beraunite $[Fe_6(OH)_6(H_2O)_3(PO_4)_4 \cdot 2H_2O]$, and cacoxenite $[Fe_4(OH)_3(PO_4)_3 \cdot 12H_2O]$ (*3*). With the exception of cacoxenite, all occur as fibrous greenish-black to brown nodules, concretions, and mammillary aggregates. Their chemical analyses often show minor and irrational amounts of ferrous iron. Single crystals of suitable dimension for crystallographic study are rare since the fibers usually consist of minute individuals in twisted bundles. Because the compositions and densities of these minerals are similar, physical, optical, or chemical characteristics alone do not suffice for certain identification. The list of species may be more extensive than the aforementioned, since Frondel documented two possibly new species and one new species is being studied in my laboratory.

Single crystals for all these species were isolated by carefully splitting fibers in acetone with a dissecting needle until an optically uniform individual could be found. Since the individuals were usually about 30 to 50 μ in mean diameter, long-exposure rotation and Weissenberg photographs were required to obtain the data reported in Table 1. Three-dimensional analysis of the crystal structure was undertaken on dufrenite and rockbridgeite (*4*). Intensity data were collected on a manual counter-diffractometer that operates on the basis of Weissenberg geometry with Zr-filtered Mo radiation for dufrenite, and on Weissenberg films with the same radiation for rockbridgeite. Atomic arrangements for these two species were determined by Patterson syntheses and vector set analysis of these data. Early refinement of atomic coordinates offers $R_{hkl} = 0.18$ (based on 1400 independent observed structure amplitudes) and 0.19 (340 independent observed structure amplitudes) for dufrenite and rockbridgeite, respectively. Their octahedral frameworks are illustrated in Fig. 1, A and B.

A remarkable polyatomic complex common to the atomic arrangements of beraunite, dufrenite, and rockbridgeite (Fig. 2) consists of an iron-oxygen

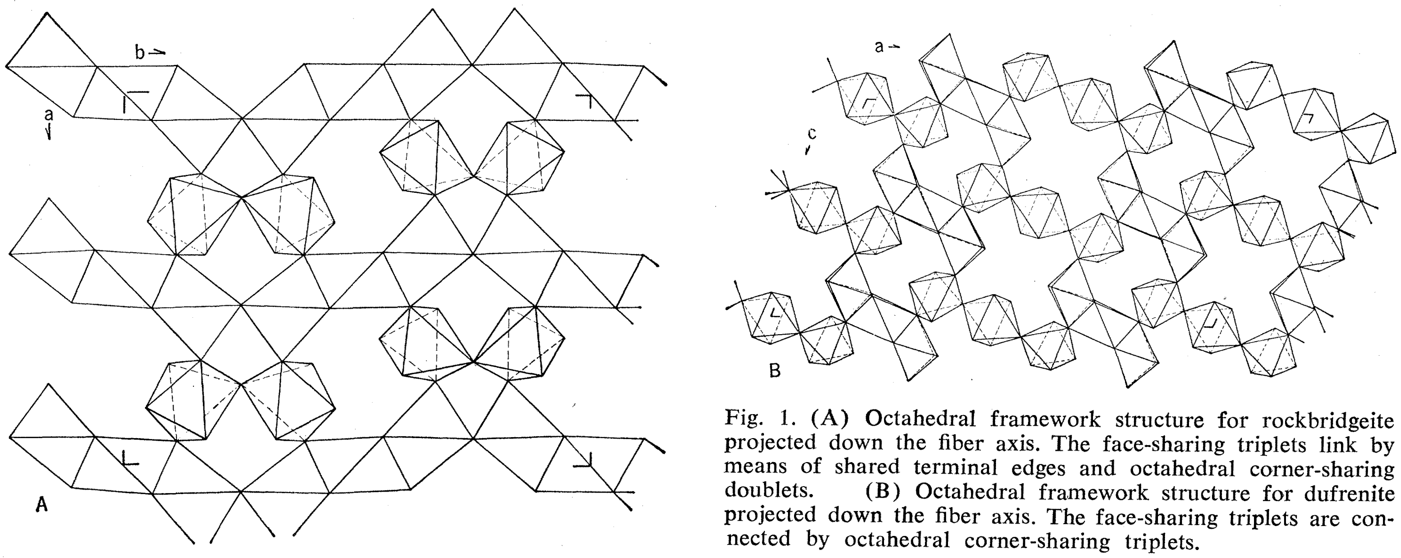

Fig. 1. (A) Octahedral framework structure for rockbridgeite projected down the fiber axis. The face-sharing triplets link by means of shared terminal edges and octahedral corner-sharing doublets. (B) Octahedral framework structure for dufrenite projected down the fiber axis. The face-sharing triplets are connected by octahedral corner-sharing triplets.